

Article

Using Geogrid Encased Granular Columns for Embankment's Slope Protection: 3D-Finite Difference Analysis

Omar Hamdi Jasim ^{1,*}  and Murat Tonaroğlu ² ¹ Department of Civil Engineering, Yildiz Technical University, 34220 Istanbul, Turkey² Department of Civil Engineering, Yildiz Technical University, Esenler, 34220 Istanbul, Turkey

* Correspondence: ojasim37@gmail.com or omar.jasim@std.yildiz.edu.tr

Abstract: The stability of the embankment's slopes is a critical aspect of geotechnical engineering and it is essential to guarantee the effectiveness of the factor of safety to prevent any potential failures in the slope both during and post-construction. The current study consists of two parts; the first part is the study of the behavior of the geogrid-encased granular columns and their interaction with the soil at the shear surface generated by the slippage of the soil, while the second part is a study of the stability of slopes by changing several factors, including the area replacement ratio (A_r %) of the granular columns, the angle of the embankment slope (β), and different elastic modulus (E_g) of geogrid on the stability of an embankment. About 90 analyses were conducted on a clayey sand embankment over a clayey layer. The area replacement ratios (A_r %) were changed by using different values of the diameter of the column; from 50 to 100 cm. The angle of the embankment slope was changed from 28 to 36 degrees. Furthermore, three different values, 0.12, 2.625, and 6.552 GPa, of modulus of elasticity were used. The results show that increasing the modulus of elasticity of the geogrid increases the normalized shear strength and decreases the lateral displacement in the column. Furthermore, the factor of safety was increased as the stiffness ratio between the geogrid and the materials increased. However, the factor of safety was noted to decrease when the angle of the embankment slope was increased.

Keywords: slope stability; factor of safety; FLAC^{3D}; granular column; geogrid; stiffness ratio



Citation: Jasim, O.H.; Tonaroğlu, M. Using Geogrid Encased Granular Columns for Embankment's Slope Protection: 3D-Finite Difference Analysis. *Appl. Sci.* **2023**, *13*, 2448. <https://doi.org/10.3390/app13042448>

Academic Editor: Daniel Dias

Received: 28 December 2022

Revised: 24 January 2023

Accepted: 5 February 2023

Published: 14 February 2023



Copyright: © 2023 by the authors. Licensee MDPI, Basel, Switzerland. This article is an open access article distributed under the terms and conditions of the Creative Commons Attribution (CC BY) license (<https://creativecommons.org/licenses/by/4.0/>).

1. Introduction

The stability of slopes is a crucial topic in the field of engineering because a failure in a slope can result in severe consequences for adjacent structures and infrastructure, therefore, in the current study, protection of slopes of an embankment was studied. The failure of the slope is mainly related to the amount of shear strength along the slip surface in the soil. Failure happens once the shear stress exceeds the shear strength of the soil. Some solutions, such as passive piles, retaining walls, soil nailing, deep mixing columns etc., have been proposed by different researchers to increase the dragging forces at the slip surface [1–7]. However, the bearing capacity and the stability of the soft soil under the embankment can also be improved by using rigid inclusions. Using geosynthetic-encased granular columns to oppose the path of the slip surface and reduce the potential failure of the slope has recently attracted the attention of some researchers. Granular columns that stabilize slopes behave similarly to passive piles [8]. Their stiffness is the main difference between them [8]. There is a piece of good evidence that granular columns have been used to increase the bearing capacity and the safety against sliding [9–14]. Vekli et al. [15] used a small-scale model to examine the effect of granular column inserted vertically in the clay and it was concluded that the factor of safety was increased by 1.18–1.62 times, also using granular columns increased the bearing capacity and decreased the settlement. Raee et al. [8] conducted an experimental and numerical analysis to study the impact of slope-stabilizing granular columns on the bearing capacity of a rigid strip footing installed

on a sand slope in which concrete piles and ordinary and encased granular columns were investigated. According to the outcomes of the study, the bearing capacity of the soil under the footing was reported to be increased as the stiffness and granular column spacing decreased. The use of geotextile-encased granular columns (GECs) as a reinforcement method for sandy slopes is a promising approach for improving slope stability. Geotextile-encased granular columns are similar to ordinary granular columns, but they are wrapped in a layer of geotextile material, which can help to improve the performance of the columns and increase their effectiveness as a reinforcement method. According to Nasiri et al. [16], the use of GECs was found to significantly increase the factor of safety of a sandy slope, with an increase of up to 37%. The GECs were also found to increase the bearing capacity of the slope foundation by 1.66 times compared to using ordinary granular columns (OGCs) without a geotextile wrap. These results suggest that GECs can be an effective way to reinforce sandy slopes and improve their stability and performance. Hajiazizi et al. [17,18] carried out a research project that compared the effectiveness of ordinary and rigid granular columns in improving the stability of sandy slopes. The findings indicated that placing the granular columns in the middle of the slope was most effective, as this is where the greatest displacements occur. The use of rigid granular columns resulted in a significant increase in the factor of safety and provided a 1.41 times greater shear strength than ordinary granular columns. Additionally, the use of rigid granular columns improved the stability of the slope by 40.6% in comparison to using only ordinary granular columns. Mohapatra et al. [19] reported that the use of GECs was found to increase the lateral load-carrying capacity of granular columns in both model and prototype scale. Furthermore, Mohapatra et al. utilized numerical modeling techniques, including three dimensional simulations with the FLAC^{3D} software [19], and the behavior of geosynthetic encased granular columns (GECs) was examined under various conditions. The findings indicated that the geosynthetic encasement of the GECs caused higher shear stresses to be mobilized within the granular column, and the magnitude of these shear stresses increased with an increase in normal pressure. Additionally, the study found that the tensile forces in the geosynthetic encasement were mobilized in both the circumferential and vertical directions, providing additional confinement to the granular column. Overall, the study suggests that GECs can be an effective way to reinforce slopes and improve their stability and bearing capacity. It is worth mentioning that, the effectiveness of GECs can depend on a variety of factors, including the soil conditions, the size and spacing of the columns, and the load conditions. It is also important to consider the costs and other practical considerations when deciding whether to use GECs in a particular project. Mohapatra and Rajagopal [20] conducted a numerical analysis to understand the behavior of inserting OGC and GEC on the embankment's stability constructed on soft clay, it was concluded that GECs contributes to increase the safety factor and the overall stability of the system. Analyzing the soil-column interaction at the slip-surface can help engineers to understand how the soil and column behave under lateral load and to design the structure appropriately, there have been a number of experimental and numerical investigations into the performance of geosynthetic encased granular columns under both horizontal and vertical loads. These studies have consistently shown that geosynthetic encased granular columns enhanced lateral load resistance and reduced lateral displacement compared to ordinary granular columns, as well as improved shear strength [21–25]. The failure mode of the columns was reported in different patterns; ordinary and encased granular columns may fail in different modes under combined horizontal and vertical loads, with failure at the center line of the embankment due to bulging and failure at the toe of the embankment due to bending or shear [9,22,26]. Researchers have devoted a significant amount of attention to the use of geosynthetic granular columns to strengthen the soil beneath embankments. However, the issue of shallow slope failure has not received as much attention. The current study aims to address this by considering slope protection for both deep-seated and shallow failure in order to enhance the stability of the embankment overall. In order to achieve the mentioned goal, two models were employed; the first model aimed to determine the

normalized shear stress of the soil and the normalized lateral displacement of the columns resulting from soil movement along the shear plane. Additionally, a slope model was simulated to analyze the impact of various factors, including the stiffness ratio between the geogrid and the soil, area replacement ratio of the granular columns, and the angle of the embankment slope on the values of factor of safety. It is widely acknowledged that the stability of embankments immediately after construction is crucial, thus short-term analysis were considered in this analysis.

2. Validation of the Numerical Model

The model has been validated based on an experimental study conducted by Mohapatra et al. [22]. A large-scale direct shear box with the dimensions of (305 mm length \times 305 mm width \times 140 mm depth) was modeled using FLAC^{3D}. The upper part of the box is fixed whereas the lower part is movable to simulate the behavior of the shear box as in the lab experiment. The shear plane is located at 76 mm from the bottom and the used soil was dense sand. A 50 mm ordinary and geosynthetic encased granular column has been constructed using rad-cylinder code at the center of the box, the geosynthetic encasement was defined as a cylinder with 1 mm thickness. Strain softening Mohr–Coulomb (SS model) was used to describe the granular column and the soil. After running the program, the model was cycled to reach the equilibrium by the self-weight. Moreover, 75 kPa of the vertical stress was applied on the upper part of the box and the model was cycled to reach the equilibrium again. The applied horizontal velocity on the lower movable part is 2×10^{-4} mm/step. 2×10^5 steps were applied to achieve a 40 mm horizontal movement. The numerical model was described in further details by Mohapatra et al. [19]. Table 1 presents the material properties adopted in the analysis. The results of the experimental study were consistent with those obtained through numerical analysis, as depicted in Figure 1.

Table 1. The characteristics of the materials used [19].

Parameter	Unit	Granular Column	Sand
Model	-	Strain softening Mohr-Coulomb	Strain softening Mohr-Coulomb
Unit weight	kN/m ³	16.2	16.3
Modulus of elasticity	MPa	100	10
Cohesion	kPa	0	0
Poisson's ratio	-	0.3	0.3
Angle of friction	Degrees	61	41
Dilation angle	Degrees	20	11

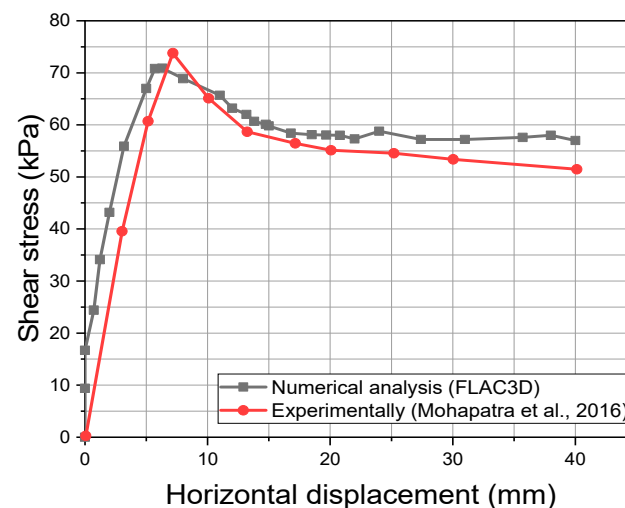


Figure 1. Shear stress- horizonal displacement curve to validate the numerical model [22].

3. Description of the Geometry and Mesh Generation

This paper consists of two parts; thus, two different models were simulated, the first model is a shear model to represent the soil-columns interaction at the shear plane. Furthermore, a slope stability model to study the effect of inserting geogrid encased columns on stability of the slope.

3.1. The First Model—Shear Model

An upper sandy soil with the dimensions of (7 m length \times 3.85 m width \times 4.5 m depth) and lower sandy soil with the dimensions of (8 m length \times 3.85 m width \times 4.5 m depth) mesh was created. Four granular columns in a square pattern with a spacing $S = 2.5D$ (center to center) were used as seen in Figures 2 and 3, where S is the spacing center to center between the columns and D is the diameter of the granular columns. The shear plane was predefined at 4.5 m from the bottom elevation to consider the worst-case scenario where the applied force has pure horizontal effects on the shear plane. By using the symmetry provided by FLAC^{3D}, a half of the above-mentioned geometry was created to minimize the time required for solutions. The extensions of the required soil were made by using a brick element. For the geogrids—6336 nodes—have been created in addition to 50,535 nodes for the soil and the granular columns. Moreover, 8736 nodes have been used to construct the interface between the sand and the geogrid. The same properties in Table 1 were used in the current study, however, different values for the angle of friction and dilation angle for the column material and the sand were used; (43, 37) and (13, 7) degrees, respectively.

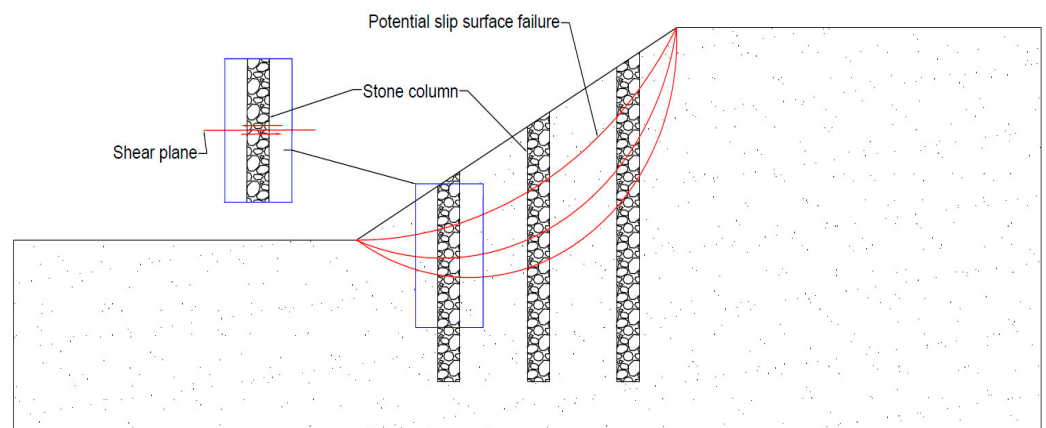


Figure 2. Slope protection by granular columns.

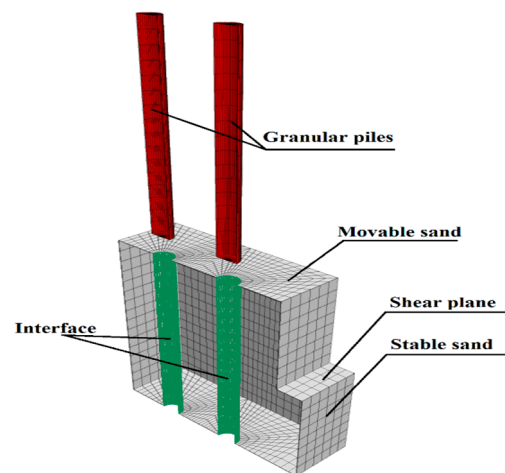


Figure 3. Cross section for geometry and mesh of the problem.

3.2. Expanding the Model—Stability of a Clayey Sand Embankment over a Clayey Soil

A clayey sand embankment constructed over a clay is considered in the present analysis. The embankment is treated and reinforced with granular columns encased with geogrid. The height of the embankment was considered to be 4.0 m. The angle of the slope of 34° (3H:2V slope). The height of clay is 4.0 m. Due to the similarity in the geometry, a half embankment was analyzed to save computation time. In this study, a single row of granular columns was analyzed to understand its behavior and effectiveness in supporting the weight of an embankment or other structure as shown in Figure 4. The granular columns were arranged in a square pattern, with a center-to-center spacing of 2.5 times the diameter of the columns. The diameter of the columns was chosen to be 1.0 m. It is important to carefully consider the boundary conditions when analyzing the behavior of a structure, as they can have a significant impact on the results. In this study, the boundary conditions were chosen such that they would not significantly affect the calculated factor of safety (FoS) value. According to Navin [27], the boundary beyond the toe of the embankment should extend at least twice the height of the embankment in order to accurately calculate the FoS. Therefore, in this study, the vertical boundary was placed 10 m beyond the toe of the embankment, ensuring that the boundary condition effects on the FoS value were minimized. To reduce the computational time and make the analysis more efficient, a bracketing solution approach was used. In this approach, if an approximate range for the FoS value is known beforehand, then the number of trials can be reduced by specifying the stable and unstable states at the beginning of the simulation. By specifying a range for the FoS value at the start of the analysis, the number of trials needed to reach a solution can be greatly reduced, making the process more efficient. The following boundary conditions are applied to the numerical models.

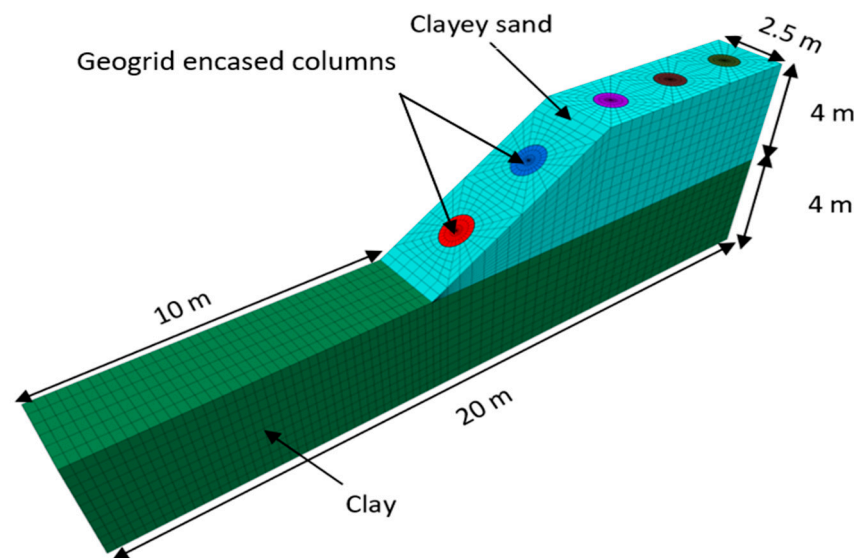


Figure 4. Details of the problem.

- (1) The bottom boundaries are fixed in all of the directions ($u_x = 0$; $u_y = 0$; $u_z = 0$);
- (2) It is assumed that the vertical boundaries are smooth $u_y = 0$, same procedure was used by [9,20,28]. The water table was assumed to be at ground surface [20].

The constitutive behavior, or the way in which a material responds to external loads, of the embankment soil, foundation soil, and granular columns was modeled using the Mohr—Coulomb model. This model is particularly well-suited for determining the factor of safety (FoS) of a slopes and embankments using the strength reduction technique. The properties of the materials were given in Table 2, and parametric studies were performed by altering the properties of the geogrid, as indicated in Table 3. To accurately represent

the granular columns and the surrounding soft soil, both a cylindrical mesh and radially graded meshes were utilized in the modeling process.

Table 2. Properties of the used materials in the FoS analysis.

Parameter	Unit	Granular Column [29]	Clayey Sand [30]	Clay [15]
Model	-	Mohr-Coulomb	Mohr-Coulomb	Mohr-Coulomb
Unit weight	kN/m ³	20	18	17
Cohesion	kPa	1	5	20
Angle of friction	Degrees	40	35	5
Angle of dilation	Degrees	10	5	0
Modulus of elasticity	MPa	50	15	5
Poisson's ratio	-	0.3	0.3	0.45

Table 3. Geogrid properties used for numerical analysis.

No.	Elastic Modulus	Unit	Poisson's Ratio	Reference
E1	0.120	GPa	0.33 *	[31]
E2	2.625	GPa	0.33 *	[32]
E3	6.552	GPa	0.33 *	[32]

* Poisson's ratio has been assumed.

4. Results and Discussion

The effect of various parameters on the factor of safety (FoS) value against slope failure of embankments constructed from clayey sand soil over clayey layer treated with granular columns is analyzed. The variables taken into account in the current analysis are area replacement ratio, angle of the embankment slope and the modulus of elasticity of the geogrid.

4.1. Soil-Column Interaction at the Slip-Surface

The effect of geogrid modulus on shear behavior-soil movement was studied using the finite differences method for different lengths of ordinary and encased granular columns ($L/D = 8, 10$ and end bearing); here L = the length of the column and D represents the diameter of the column. Figures 5–7 explain the variations of the normalized shear stress (which is the shear stress after improvement divided by the shear stress of the soil (τ_{imp}/τ_{soil})), with the normalized soil movement ((δ/D) where δ is the lateral soil movement) behavior of sand improved with ordinary granular columns (OGC) and geogrid encased granular columns (GECs). Different values of the modulus of elasticity have been used in the analysis as shown in Table 3. It concluded that increasing the modulus of elasticity of geogrid contributes to increasing the overall resistance of the soil against lateral movement especially at the shear plane as shown in Figures 5a, 6a and 7a, the reason behind that is the overall stiffness of the granular columns was increased [21,22,33]. The use of geogrid encased columns can also improve the load distribution in the soil, which can lead to a reduction in the shear stress on soil particles [33,34]. It was noticed that the largest effect of geogrid occurred on end bearing geogrid encased granular columns. The values of shear strength were increased by (17.7)%. Furthermore, it was found that the geogrid has a positive effect on the value of the lateral displacement of the column. Increasing the modulus of elasticity of the geogrid led to an increase in the overall resistance to lateral displacement as shown in Figures 5b, 6b and 7b.

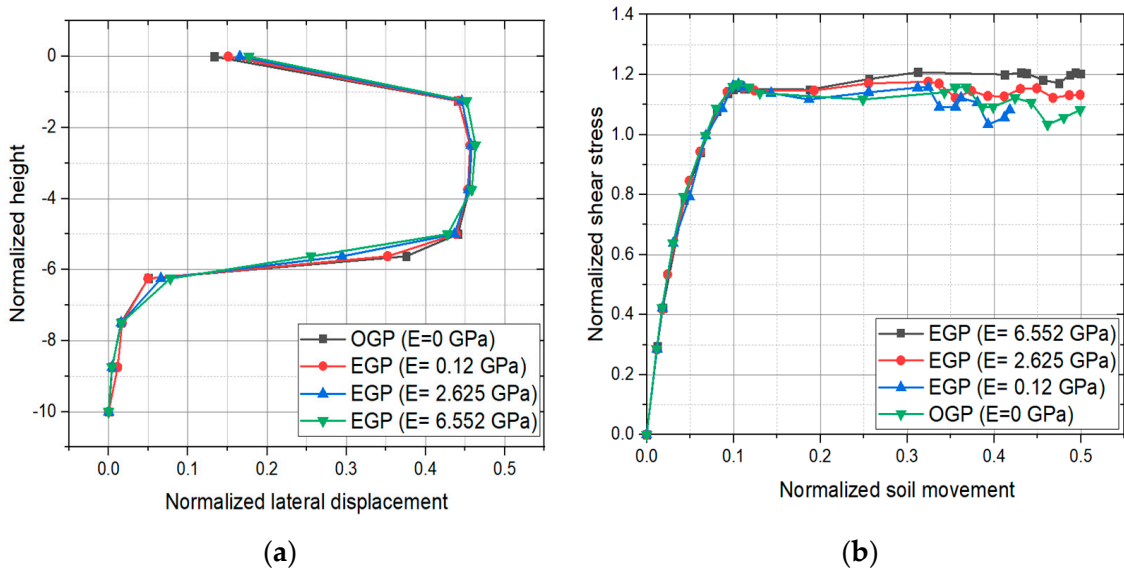


Figure 5. Soil—column interaction at the shear plane. (a) Normalized height vs. normalized lateral displacement. (b) Normalized shear strength vs. normalized soil movement in end bearing columns.

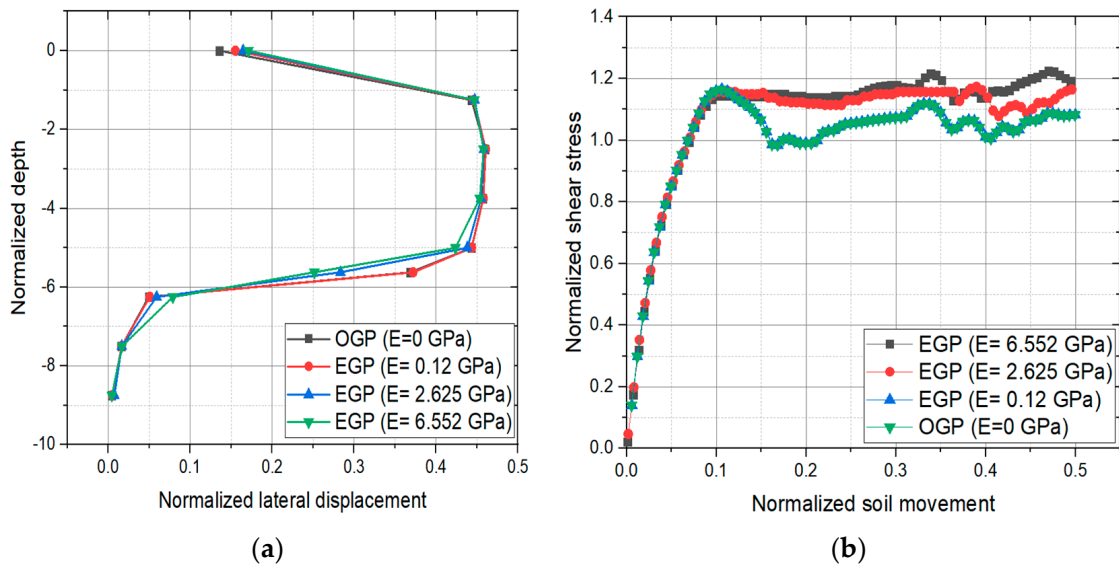


Figure 6. Soil—column interaction at the shear plane. (a) Normalized height vs. normalized lateral displacement. (b) Normalized shear strength vs. normalized soil movement in embedment ratio $L/D = 10$.

4.2. Effect of Area Replacement Ratio (A_r %) of the Granular Columns on the Factor of Safety (FoS)

The current analysis examined the impact of varying the diameter of granular columns on the factor of safety (FoS). Seven diameters (50, 60, 70, 80, 90, and 100 cm) were selected, representing 5.815–11.63% area replacement ratio. Results showed that using low elastic modulus geogrid ($E = 0.120$ GPa) resulted in an average 13% increase in FoS across all embankment angles (as seen in Figure 8a). Using medium strength elastic modulus geogrid ($E = 2.625$ GPa) led to a 20% increase in FoS compared to the low elastic modulus geogrid (Figure 8b). Additionally, the contribution of encasement to FoS values decreased as the embankment angle increased (Figure 8c). Using high modulus geogrid had a very minor effect on FoS compared to medium strength elastic modulus. The findings suggest that increasing the area replacement ratio improves slope stability by increasing the shear resistance and dissipating energy generated by soil movement. This is achieved

by increasing the sheared area, which reduces the distribution of shear forces and strains along the failure line [20,25,35]. Fattah and Majeed [11] found that increasing the area replacement ratio significantly improved the bearing capacity of encased floating stone columns, especially when the area replacement ratio exceeded 0.25. They also observed that using a geogrid encasement significantly reduced lateral displacement compared to using ordinary stone columns.

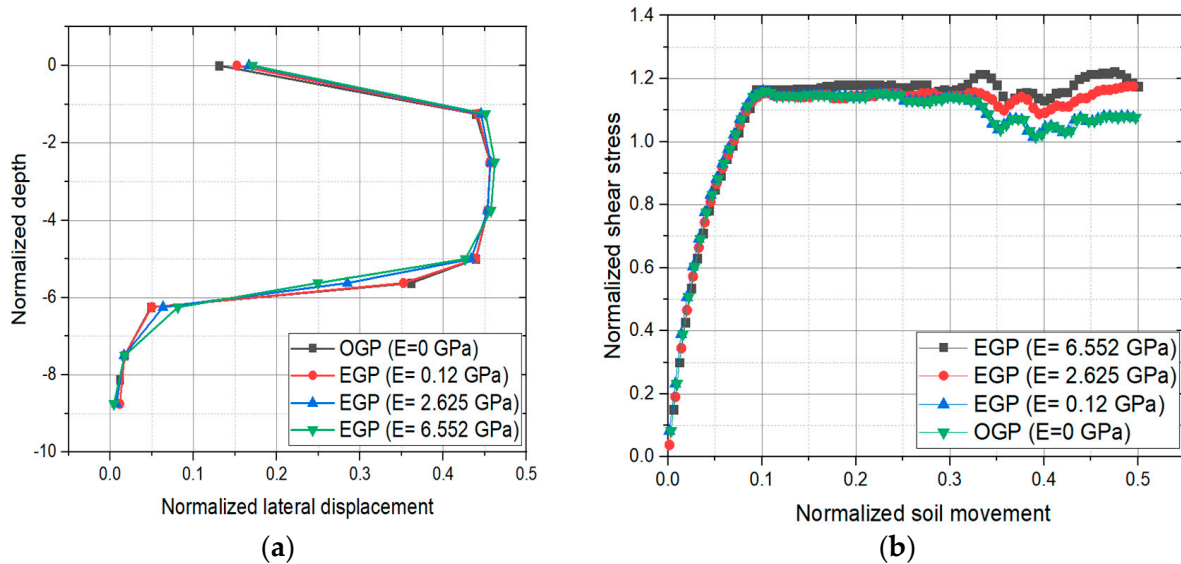


Figure 7. Soil—column interaction at the shear plane. (a) Normalized height vs. normalized lateral displacement. (b) Normalized shear strength vs. normalized soil movement in embedment ratio $L/D = 8$.

4.3. The Relationship between Stability Number (m) and Factor of Safety (FoS)

The stability number is a dimensionless parameter that is used to evaluate the stability of an embankment against failure. The value of the stability number was calculated as follows

$$m = \frac{c}{\gamma \times H}$$

where (c) is the cohesion of the embankment soil, (γ) is the unit weight of the soil and (H) is the height of the slope.

The variation of the factor of safety (FoS) of a clayey sand embankment with the stability number (m) for various geogrid elastic moduli (E) at various values of the slope angle (β) is addressed in Figure 9a–c. It has been observed that the factor of safety (FoS) tends to rise linearly as the stability number (m) increases. Furthermore, it is discovered that the FoS is inversely proportional to the slope angle (β), which means that a rise in the slope angle causes a fall in the FoS [36].

4.4. Effect of Material’s Stiffness Ratio on the Factor of Safety (FoS)

The stiffness ratio represents the different characteristics between the stiffness of the geogrid with respect to the stiffness of the materials. In this study, the elastic modulus of embankment (E_m), clay (E_c) and the granular columns (E_{col}) was kept constant, and the stiffness of the geogrid (E_g) was changed (Table 3) to represent the stiffness ratio corresponding to each one of them as follows, E_g/E_m , E_g/E_c , and E_g/E_{col} , respectively.

Figures 10–12 show that at the relatively high angle of embankment slope (β). It was observed that factor of safety (FoS) values increases with an increase in the stiffness ratio of the geogrid with respect to the other materials (i.e., embankment, clay, and column). On the other hand, very minor effect for the area replacement ratio (Ar %) was recorded on the factor of safety in the high stiffness values. At low angle of embankment slope (β) values, the stiffness ratio values have led to positive effects on the stability of the

embankment. The amount of increase (as comparing to high β values) was found to be higher. The reason behind this is that the geogrid increases the length of the slip surface and increases the friction along the shear plane. Furthermore, in high stiffness values, the geogrid granular columns GECs contribute to delay the plastic (yielding behavior) in the soil [8] by mobilizing higher forces (stresses) [22].

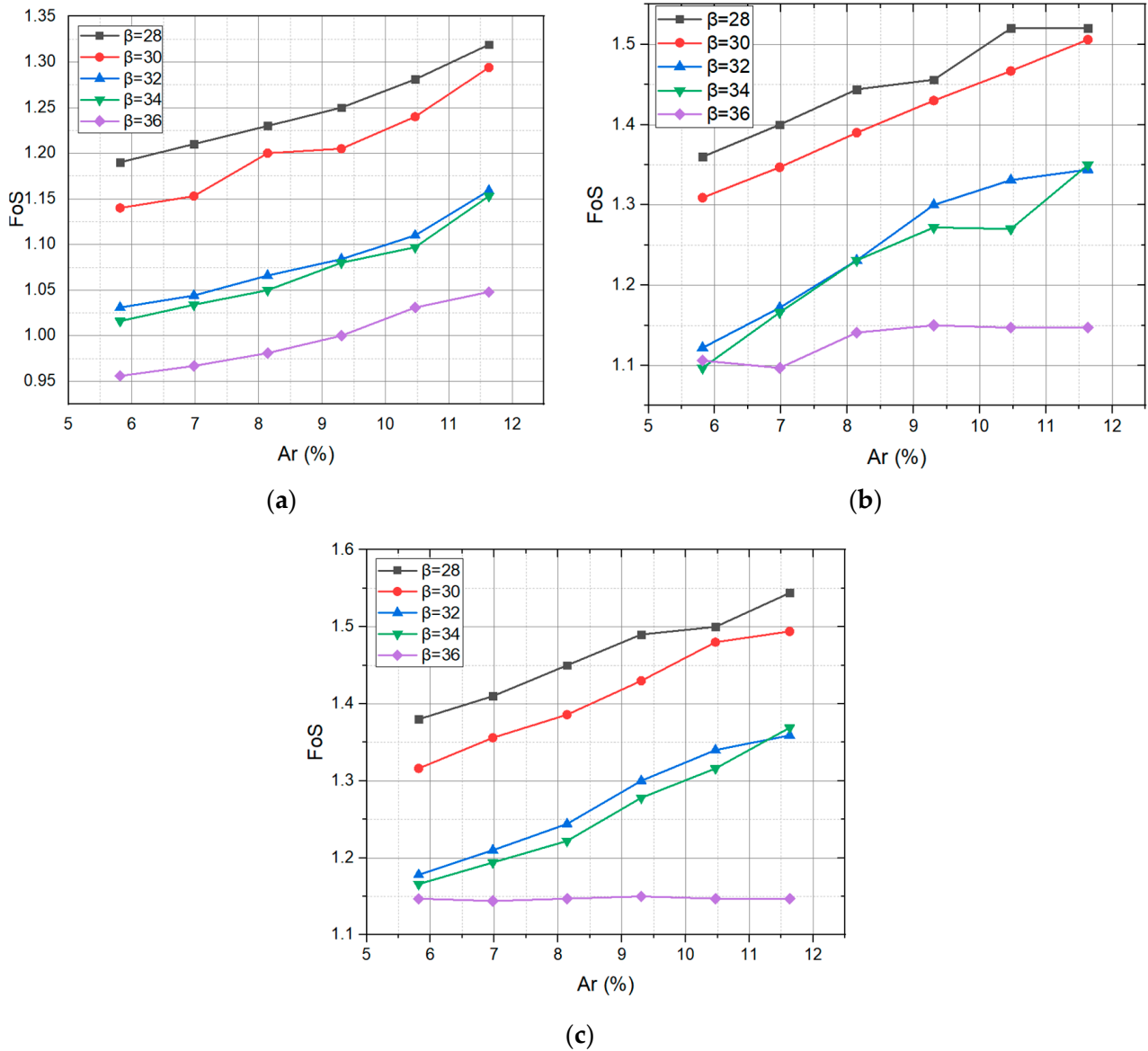


Figure 8. Effect of area replacement ratio (Ar %) on factor of safety using (a) E1 of geogrid = 0.12 GPa (b) E2 of geogrid = 2.625 and (c) E3 of geogrid = 6.552 GPa.

4.5. Failure Mode of the Geogrid Encased Granular Columns

As reported in Figure 13, the failure mode identified in the slope prior to reinforcement was deep-seated slope failure. Inserting of ordinary and geogrid encased granular columns contributed to changing the type of failure from deep-seated failure to shallow slope failure with higher factor of safety. Further analysis revealed that the OGCs reinforcing the slope failed due to bending, while the OGCs reinforcing the body of the embankment failed as a result of bulging [9,20,23], as shown in Figure 14. On the other hand, GECs (geogrid encased columns) failed due to bending failure. Increasing the stiffness of the geogrid decreases the bending failure of the column. Granular columns at the embankment’s centerline experienced substantially lower lateral movement compared to those supporting

the inclined portion of the embankment (the toe). More pronounced lateral displacements were seen in the GECs on the slope than in the embankment’s body. The column—soil system’s overall stiffness tends to rise due to the confinement effect given by the geogrid encasement. Thus, the safety of the slopes generally increases. The surface settlement of the embankment was found to be improved during using geogrid encased granular columns as shown in Figure 15.

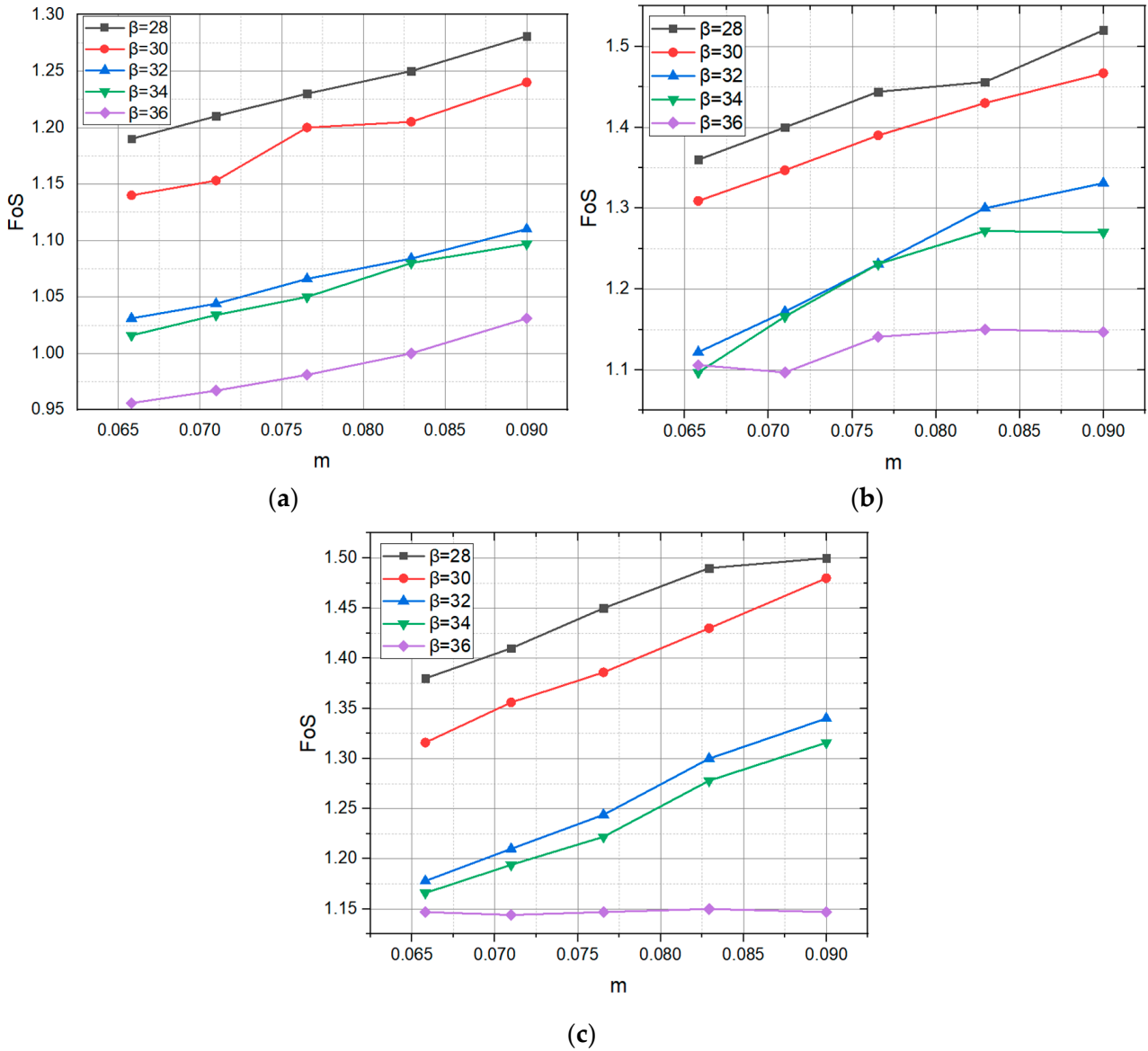


Figure 9. The relationship between stability number and factor of safety (a) $E1$ of geogrid = 0.12 GPa (b) $E2$ of geogrid = 2.625 GPa and (c) $E3$ of geogrid = 6.552 GPa.

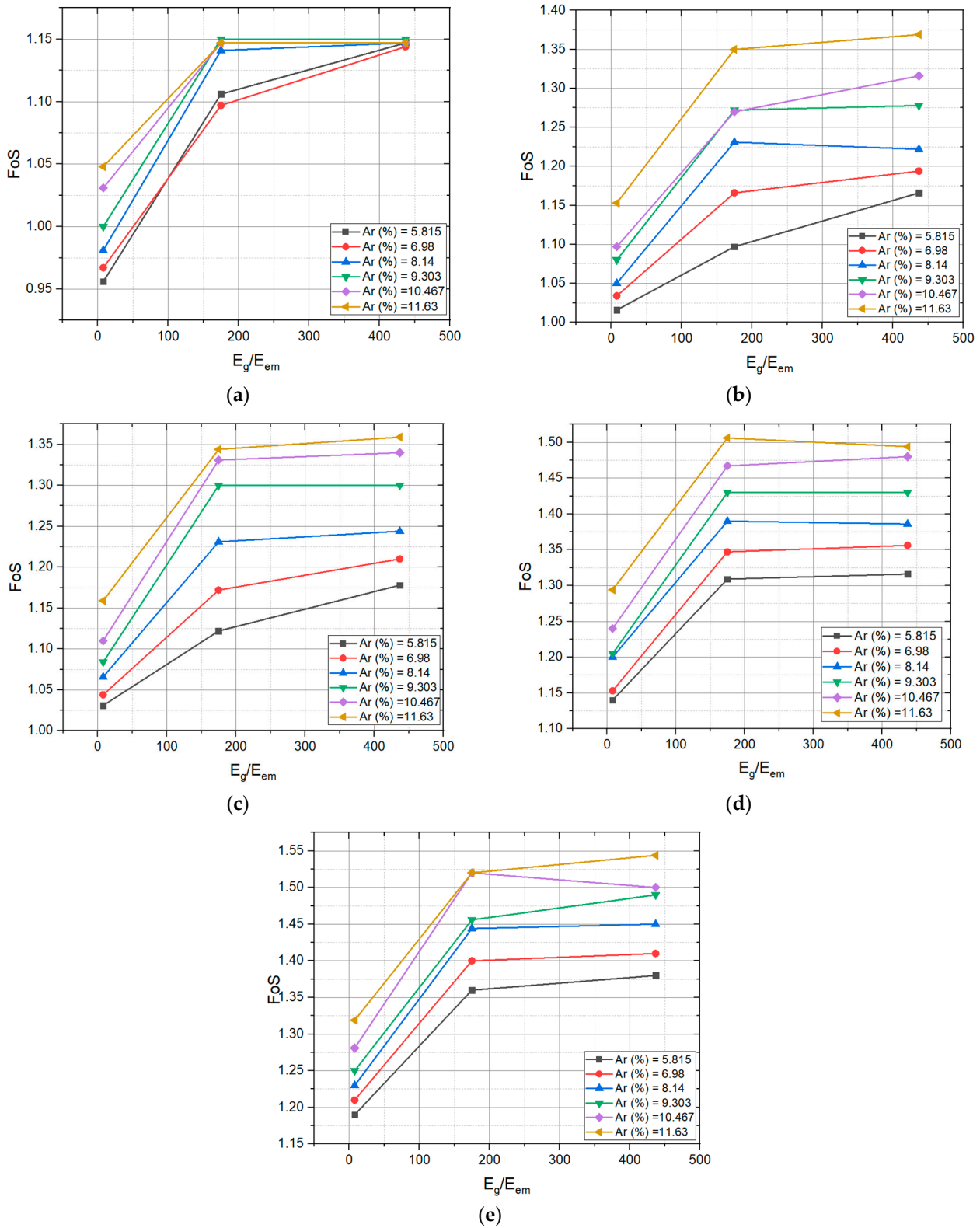


Figure 10. Effect of $E_{geogrid}/E_{embankment}$ (E_g/E_{em}) stiffness ratio on (FoS) for (a) $\beta = 36$, (b) $\beta = 34$, (c) $\beta = 32$ (d) $\beta = 30$ and (e) $\beta = 28$.

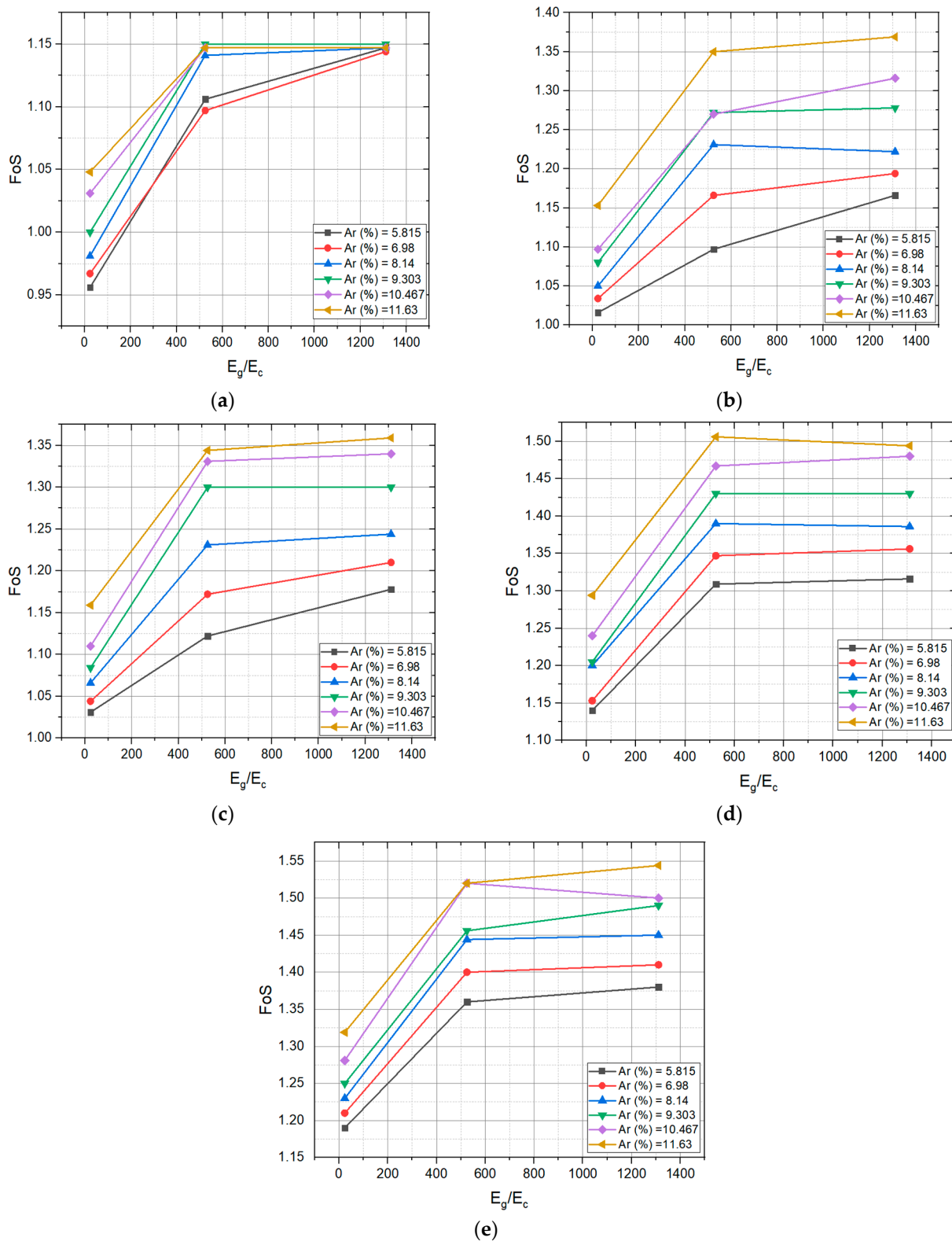


Figure 11. Effect of $E_{geogrid}/E_{clay}$ (E_g/E_c) stiffness ratio on (FoS) for (a) $\beta = 36$, (b) $\beta = 34$, (c) $\beta = 32$ (d) $\beta = 30$ and (e) $\beta = 28$.

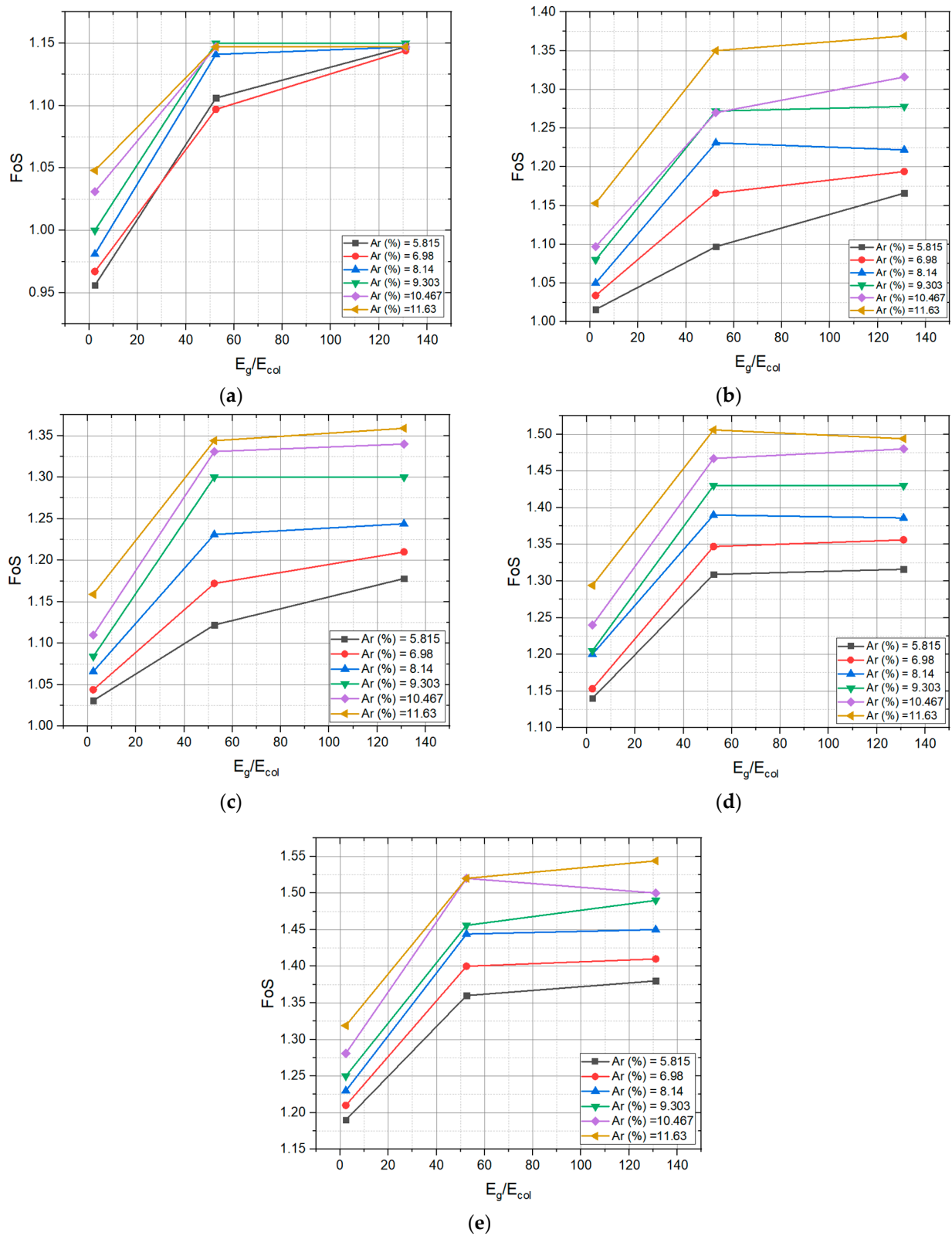


Figure 12. Effect of $E_{geogrid}/E_{column}$ (E_g/E_{col}) stiffness ratio on (FoS) for (a) $\beta = 36$, (b) $\beta = 34$, (c) $\beta = 32$ (d) $\beta = 30$ and (e) $\beta = 28$.

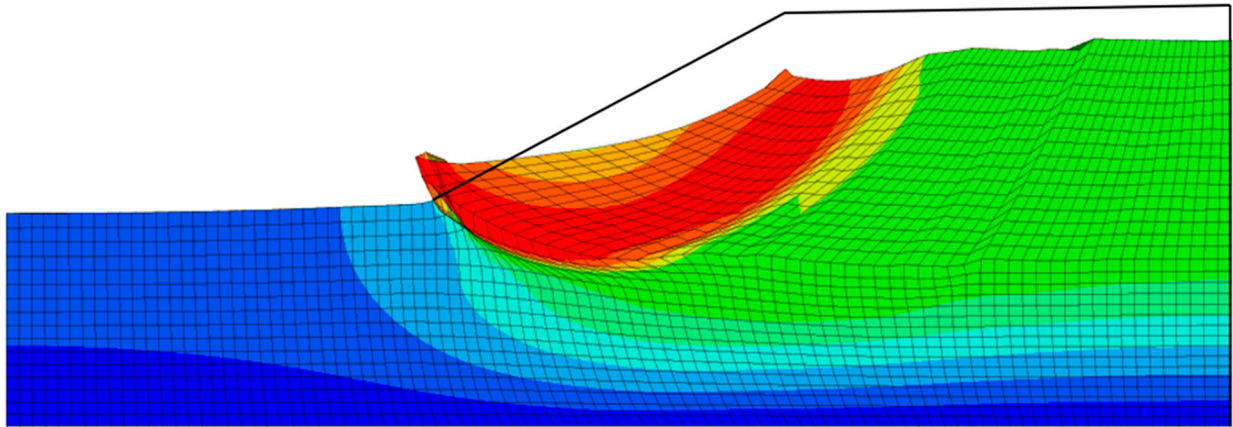


Figure 13. The failure mode in the slope of the embankment before the reinforcement with geogrid encased columns.

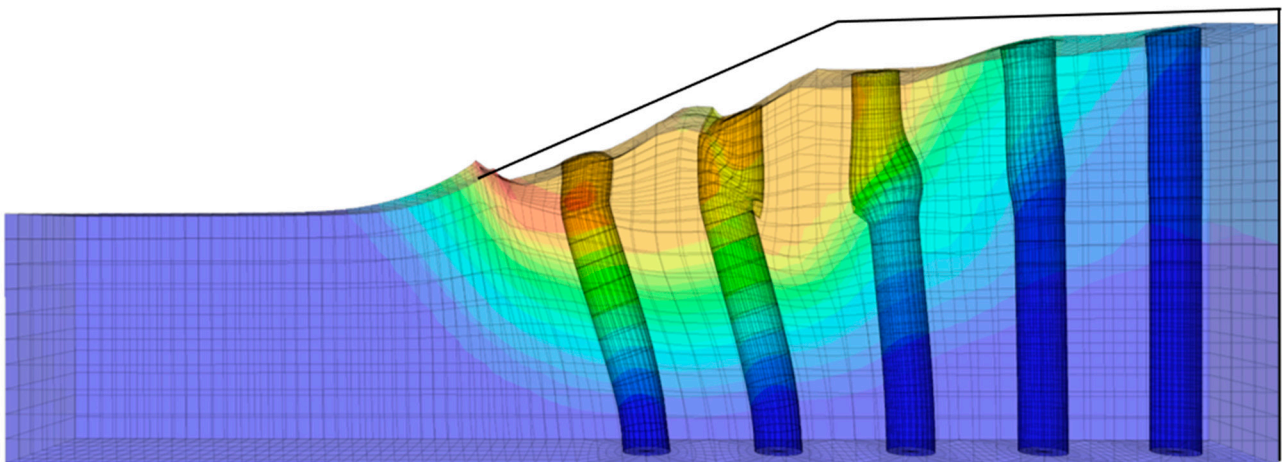


Figure 14. Failure modes of ordinary granular columns.

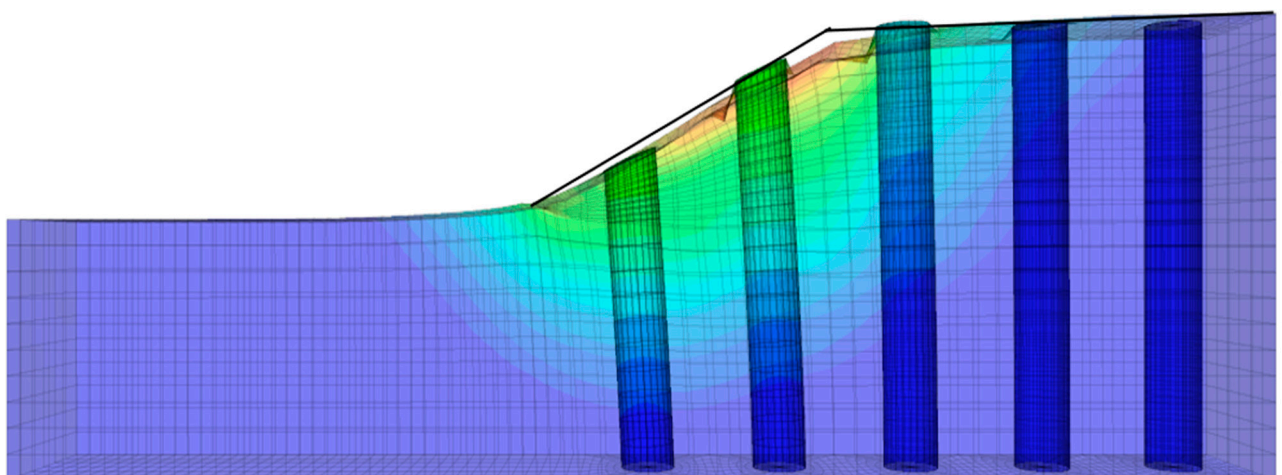


Figure 15. Bending failure mode in the geogrid encased columns.

5. Conclusions

The current study is a three-dimensional finite-difference analysis on the effect of inserting GECs on the shear behavior of the soil, with a particular emphasis on the use of GECs to improve stability under different scenarios. through changes in various factors

such as the area replacement ratio of granular columns, the angle of the embankment slope, and different elastic moduli of geogrid. The analyses were conducted on a clayey sand embankment over a clayey layer. The results indicate that increasing the modulus of elasticity of the geogrid leads to an increase in normalized shear strength and a decrease in lateral displacement in the column. Additionally, the factor of safety increases as the stiffness ratio between the geogrid and the materials increases. However, the factor of safety decreases as the angle of the embankment slope increases. The following points can be concluded:

- Using geogrid encased granular columns (GECs) can significantly increase the shear strength along the failure plane. The geogrid acts as a reinforcement material that helps to distribute more load and prevent failure.
- The angle of the embankment plays a critical role in determining the failure mode of the slope. As the angle decreases, the failure mode shifts from deep seated, to face failure. This is due to the fact that at lower angles, the soil is less likely to slide.
- The modulus of elasticity of the geogrid can also impact the performance of GECs. At very high modulus of elasticity, the effect of area replacement ratio on the value of factor of safety, is minimal.
- As the angle of the embankment slope decreases, the performance of GECs improves.
- The margin of safety increases as the stability number (m) increases. A higher stability number indicates a more stable slope.
- It is generally not recommended to use GECs for slope protection if the angle of the slope is more than 34 degrees with the horizontal. This is because at steeper angles the soil is more likely to move, and GECs is not effective in preventing failure.
- It was found that the most significant factors affecting the factor of safety are the angle of the slope of the embankment, the modulus of elasticity of the geogrid, the area replacement ratio, and the stability number respectively. These factors were found to have the greatest impact on the overall safety and stability of the embankment.

Author Contributions: Conceptualization, O.H.J. and M.T.; methodology, O.H.J. and M.T.; software, O.H.J.; validation, O.H.J.; formal analysis, O.H.J.; investigation, O.H.J. and M.T.; resources, O.H.J. and M.T.; data curation, O.H.J.; writing—original draft preparation, O.H.J.; writing—review and editing, O.H.J. and M.T.; visualization, O.H.J.; supervision M.T.; project administration, M.T. All authors have read and agreed to the published version of the manuscript.

Funding: This research received no external funding.

Institutional Review Board Statement: Not applicable.

Informed Consent Statement: Not applicable.

Data Availability Statement: Not applicable.

Conflicts of Interest: The authors declare no conflict of interest.

References

1. Poulos, H.G.; Chen, L.T.; Hull, T.S. Model tests on single piles subjected to *Lateral* soil movement. *Soils Found* **1995**, *35*, 85–92. [[CrossRef](#)] [[PubMed](#)]
2. Han, J.; Oztoprak, S.; Parsons, R.L.; Huang, J. Numerical analysis of foundation columns to support widening of embankments. *Comput. Geotech.* **2007**, *34*, 435–448. [[CrossRef](#)]
3. Li, J.; Tham, L.G.; Junaideen, S.M.; Yue, Z.Q.; Lee, C.F. Loose Fill Slope Stabilization with Soil Nails: Full-Scale Test. *J. Geotech. Geoenviron. Eng.* **2008**, *134*, 277–288. [[CrossRef](#)]
4. Low, B.K.; Zhang, J.; Tang, W.H. Efficient system reliability analysis illustrated for a retaining wall and a soil slope. *Comput. Geotech.* **2011**, *38*, 196–204. [[CrossRef](#)]
5. Zhang, G.; Cao, J.; Wang, L. Centrifuge model tests of deformation and failure of nailing-reinforced slope under vertical surface loading conditions. *Soils Found* **2013**, *53*, 117–129. [[CrossRef](#)]
6. Ye, G.; Cai, Y.; Zhang, Z. Numerical study on load transfer effect of Stiffened Deep Mixed column-supported embankment over soft soil. *KSCE J. Civ. Eng.* **2017**, *21*, 703–714. [[CrossRef](#)]

7. Galli, A.; Salice, M.; Becci, B. Analytical Solutions for Ultimate Stabilizing Action of Anchored Piles in Cohesive Soil Layers. *Int. J. Geomech.* **2022**, *22*, 1–11. [[CrossRef](#)]
8. Raei, E.; Hataf, N.; Barkhordari, K.; Ghahramani, A. The Effect of Rigidity of Reinforced Stone Columns on Bearing Capacity of Strip Footings on the Stabilized Slopes. *Int. J. Civ. Eng.* **2019**, *17*, 673–685. [[CrossRef](#)]
9. Abusharar, S.W.; Han, J. Two-dimensional deep-seated slope stability analysis of embankments over stone column-improved soft clay. *Eng. Geol.* **2011**, *120*, 103–110. [[CrossRef](#)]
10. Fattah, M.Y.; Majeed, Q.G. Finite Element Analysis of Geogrid Encased Stone Columns. *Geotech. Geol. Eng.* **2012**, *30*, 713–726. [[CrossRef](#)]
11. Mohanty, P.; Samanta, M. Experimental and Numerical Studies on Response of the Stone Column in Layered Soil. *Int. J. Geosynth. Ground Eng.* **2015**, *1*, 1–14. [[CrossRef](#)]
12. Fattah, M.Y.; Zabar, B.S.; Hassan, H.A. Experimental Analysis of Embankment on Ordinary and Encased Stone Columns. *Int. J. Geomech.* **2016**, *16*, 1–13. [[CrossRef](#)]
13. Fattah, M.Y.; Al-Neami, M.A.; Shamel Al-Suhaily, A. Estimation of bearing capacity of floating group of stone columns. *Eng. Sci. Technol. Int. J.* **2017**, *20*, 1166–1172. [[CrossRef](#)]
14. Grizi, A.; Al-Ani, W.; Wanatowski, D. Numerical Analysis of the Settlement Behavior of Soft Soil Improved with Stone Columns. *Appl. Sci.* **2022**, *12*, 5293. [[CrossRef](#)]
15. Vekli, M.; Aytekin, M.; Banu İkizler, S.; Çalik, Ü. Experimental and numerical investigation of slope stabilization by stone columns. *Nat. Hazards* **2012**, *64*, 797–820. [[CrossRef](#)]
16. Nasiri, M.; Hajiazizi, M. An experimental and numerical investigation of reinforced slope using geotextile encased stone column. *Int. J. Geotech. Eng.* **2019**, 1–10. [[CrossRef](#)]
17. Hajiazizi, M.; Nasiri, M. Experimental and numerical study of earth slope reinforcement using ordinary and rigid stone columns. *Int. J. Min. Geo-Eng.* **2018**, *52*, 23–30. [[CrossRef](#)]
18. Hajiazizi, M.; Nasiri, M. Earth Slopes Reinforced by Stone Column and Geotextile. *Geotech. Eng.* **2019**, *46*, 5828.
19. Mohapatra, S.R.; Rajagopal, K.; Sharma, J. 3-Dimensional numerical modeling of geosynthetic-encased granular columns. *Geotext. Geomembr.* **2017**, *45*, 131–141. [[CrossRef](#)]
20. Mohapatra, S.R.; Rajagopal, K. Undrained stability analysis of embankments supported on geosynthetic encased granular columns. *Geosynth. Int.* **2017**, *24*, 465–479. [[CrossRef](#)]
21. Murugesan, S.; Rajagopal, K. Shear load tests on stone columns with and without geosynthetic encasement. *Geotech. Test. J.* **2009**, *32*, 76–85.
22. Mohapatra, S.R.; Rajagopal, K.; Sharma, J. Direct shear tests on geosynthetic-encased granular columns. *Geotext. Geomembr.* **2016**, *44*, 396–405. [[CrossRef](#)]
23. Cengiz, C.; Kilic, I.E.; Guler, E. On the shear failure mode of granular column embedded unit cells subjected to static and cyclic shear loads. *Geotext. Geomembr.* **2019**, *47*, 193–202. [[CrossRef](#)]
24. Naeini, S.A.; Gholampoor, N. Effect of Geotextile Encasement on the Shear Strength Behavior of Stone Column-Treated Wet Clays. *Indian Geotech. J.* **2019**, *49*, 292–303. [[CrossRef](#)]
25. Hosseinpour, I.; Ghorbani, A.; Zarei, J.; Ranjan Mohapatra, S. Experimental study on the behaviour of granular column-treated soft clay under shear loading. *Geomech. Geoengin.* **2022**, 1–12. [[CrossRef](#)]
26. Chen, J.F.; Li, L.Y.; Xue, J.F.; Feng, S.Z. Failure mechanism of geosynthetic-encased stone columns in soft soils under embankment. *Geotext. Geomembr.* **2015**, *43*, 424–431. [[CrossRef](#)]
27. Navin, M.P. Stability of Embankments Founded on Soft Soil Improved with Deep-Mixing-Method Columns. *Psychol. Sci.* **2005**, *25*, 1682–1690.
28. Zheng, G.; Yu, X.; Zhou, H.; Wang, S.; Zhao, J.; He, X.; Yang, X. Stability analysis of stone column-supported and geosynthetic-reinforced embankments on soft ground. *Geotext. Geomembr.* **2020**, *48*, 349–356. [[CrossRef](#)]
29. Zahmatkesh, A.; Choobbasti, A.J. Settlement evaluation of soft clay reinforced with stone columns using the equivalent secant modulus. *Arab. J. Geosci.* **2012**, *5*, 103–109. [[CrossRef](#)]
30. Bergado, D.T.; Alfaro, M.C.; Chai, J.C.; Balasubramaniam, A.S.; Shivashankar, R. Interaction behaviour of steel grid reinforcements in a clayey sand. *Geotechnique* **1993**, *43*, 589–603. [[CrossRef](#)]
31. Hussein, M.G.; Meguid, M.A. A three-dimensional finite element approach for modeling biaxial geogrid with application to geogrid-reinforced soils. *Geotext. Geomembr.* **2016**, *44*, 295–307. [[CrossRef](#)]
32. Dong, Y.L.; Han, J.; Bai, X.H. Numerical analysis of tensile behavior of geogrids with rectangular and triangular apertures. *Geotext. Geomembr.* **2011**, *29*, 83–91. [[CrossRef](#)]
33. Nazariafshar, J.; Aslani, M. Effect of Stress Concentration Ratio on Shear Strength of Soft Soils Improved with Stone Columns. *Iran. J. Sci. Technol.—Trans Civ. Eng.* **2020**, *45*, 315–334. [[CrossRef](#)]
34. Fattah, M.Y.; Shlash, K.T.; Al-Waily, M.J. Experimental evaluation of stress concentration ratio of model stone columns strengthened by additives. *Int. J. Phys. Model. Geotech.* **2013**, *13*, 79–98. [[CrossRef](#)]

35. Jiang, Y.; Han, J.; Zheng, G. Numerical analysis of consolidation of soft soils fully-penetrated by deep-mixed columns. *KSCE J. Civ. Eng.* **2013**, *17*, 96–105. [[CrossRef](#)]
36. Abdalla, J.A.; Attom, M.F.; Hawileh, R. Prediction of minimum factor of safety against slope failure in clayey soils using artificial neural network. *Environ. Earth Sci.* **2015**, *73*, 5463–5477. [[CrossRef](#)]

Disclaimer/Publisher’s Note: The statements, opinions and data contained in all publications are solely those of the individual author(s) and contributor(s) and not of MDPI and/or the editor(s). MDPI and/or the editor(s) disclaim responsibility for any injury to people or property resulting from any ideas, methods, instructions or products referred to in the content.